

## A dual-resonant terahertz metamaterial based on single-particle electric-field-coupled resonators

Yu Yuan,<sup>1</sup> Christopher Bingham,<sup>2</sup> Talmage Tyler,<sup>1</sup> Sabarni Palit,<sup>1</sup> Thomas H. Hand,<sup>1</sup> Willie J. Padilla,<sup>2</sup> Nan Marie Jokerst,<sup>1</sup> and Steven A. Cummer<sup>1,a)</sup>

<sup>1</sup>Department of Electrical and Computer Engineering, Duke University, Durham, North Carolina 27708, USA

<sup>2</sup>Department of Physics, Boston College, Chestnut Hill, Massachusetts 02467, USA

(Received 21 July 2008; accepted 22 October 2008; published online 13 November 2008)

We report the design, fabrication, and measurement of a terahertz metamaterial composed of single geometry electric field coupled resonators that has two closely spaced electric resonances near 1.0 and 1.5 THz. Due to the mutual coupling between the different resonances in the particle, the lower frequency resonance of this metamaterial is stronger than that in a metamaterial composed of identically sized single-resonant particles, leading to a larger insertion loss and broader bandwidth. This feature provides more flexibility in metamaterial design and application in the terahertz regime. © 2008 American Institute of Physics. [DOI: 10.1063/1.3026171]

Since the experimental demonstration of negative refractive index materials,<sup>1</sup> metamaterial research has attracted intense attention of the scientific community. Metamaterials composed of conventional metallic wires,<sup>2</sup> split-ring resonators (SRRs),<sup>3</sup> and their variation, such as S-shaped and double S-shaped resonators,<sup>4,5</sup> and electric-field-coupled (ELC) resonators<sup>6</sup> were first designed and fabricated in the microwave frequency regime. ELC resonators, which do not require continuous connections between unit cells,<sup>6</sup> are scalable and can be patterned on a planar structure to realize an electric response. These features are particularly desirable for constructing microwave invisibility cloaks<sup>7</sup> and functional materials in the terahertz regime.<sup>8,9</sup>

Design and fabrication of multiresonant metamaterials are potentially useful and thus are attractive. A microwave dual-band negative-index metamaterial was fabricated and experimentally confirmed,<sup>10</sup> and found its application in a multifrequency resonator.<sup>11</sup> Recently, near-infrared metamaterials with dual-band negative-index characteristics were also reported.<sup>12,13</sup> Motivated by the application of metamaterials fill the terahertz gap, a dual-band planar electric metamaterial was designed and fabricated in the terahertz regime using two different sized symmetrical SRRs.<sup>14</sup> We demonstrate here an ELC-resonator based metamaterial composed of particles of a single geometry that has two distinct resonances near 1.0 and 1.5 THz. The ELC resonator is composed of two different single-resonant ELCs that have the same capacitorlike gaps that couple to the electrical field, but with different inductive loops to excite two distinct LC resonances. Remarkably, comparison of this metamaterial to its single-resonance counterparts demonstrates that due to the coupling between the different single-resonant particles within the structure, the performance of its first resonance, including the transmission minimum, and the bandwidth of the stop band near resonance, can be significantly enhanced.

Two single-resonant particles are first designed with the resonances near 1.0 and 1.5 THz, and then are integrated into a single particle. All the designs were performed utilizing *Ansoft* HFSS, a commercial electromagnetic solver based on

the finite element method. The designed dual-resonant particle is shown in Fig. 1 (left), with its geometrical parameters described in the caption. The resonator composed of titanium, platinum, and gold layers (the thicknesses of Ti/Pt/Au: 30/40/200 nm), and the 50- $\mu\text{m}$ -thick gallium arsenide (GaAs) substrate, with a real permittivity of 12.8 and a loss tangent of 0.006,<sup>14</sup> are modeled. A method based on viewing the planar metamaterial as multilayer system, which was validated in previous work,<sup>14</sup> is adopted to calculate the transmission of the metamaterial sample. As is shown in Fig. 2(a) (blue line), two transmission minima are expected at 0.92 and 1.39 THz, respectively, and the calculated peak between them is centered at 1.25 THz. The calculated transmission minima near the two resonances are 0.8% and 13.5%, respectively, and the transmission at the peak between the two resonances is 42.3%. The metamaterial is characterized by retrieval methods described in Refs. 15 and 16, assuming that a 10  $\mu\text{m}$  metamaterial layer is stacked repeatedly along the wave propagation direction. The retrieved permittivity is shown in Fig. 2(b), in which our  $\exp(+j\omega t)$  time convention means that the negative imaginary permittivity implies loss. Note the high background permittivity of the metamaterial because of the intrinsic permittivity of GaAs. The strong amplitude difference between the resonances is discussed below.

The planar array of the designed ELC resonators with a lattice constant of 50  $\mu\text{m}$  were fabricated on the GaAs sub-

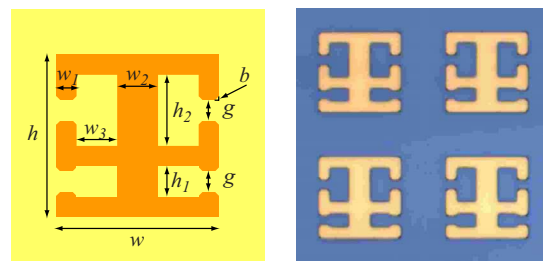


FIG. 1. (Color online) (Left) designed unit cell, with geometries:  $h=w=32\ \mu\text{m}$ ,  $w_1=4\ \mu\text{m}$ ,  $w_2=8\ \mu\text{m}$ ,  $w_3=8\ \mu\text{m}$ ,  $h_1=8\ \mu\text{m}$ ,  $h_2=14\ \mu\text{m}$ ,  $g=4\ \mu\text{m}$ , and  $b=0.8\ \mu\text{m}$ . (Right) Photomicrograph of the fabricated sample. The lattice constant of the unit cell is 50  $\mu\text{m}$ .

<sup>a)</sup>Electronic mail: cummer@ee.duke.edu.

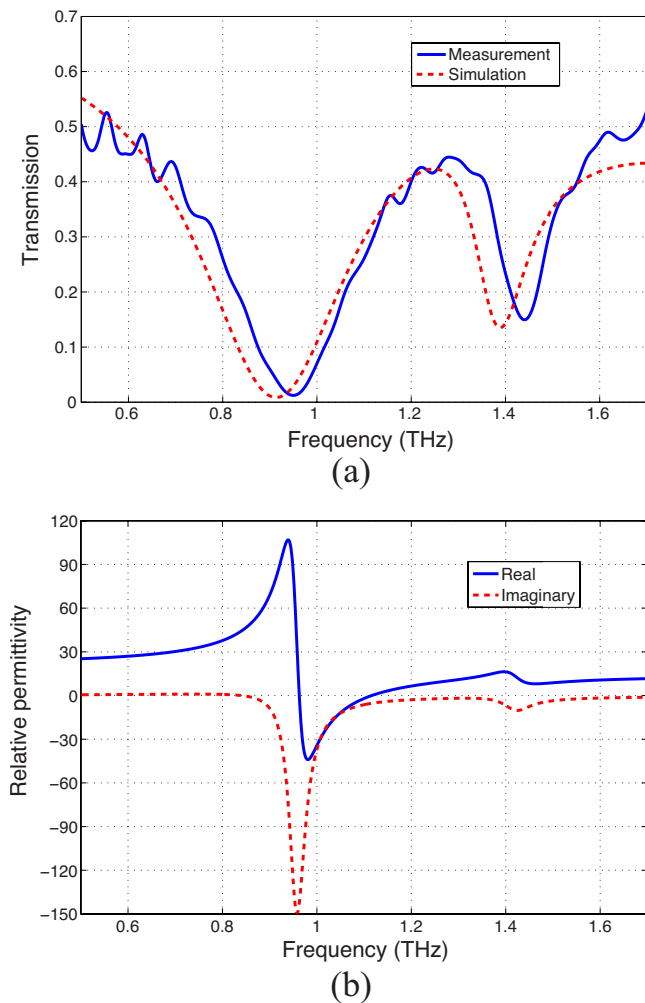


FIG. 2. (Color online) (a) Calculated (blue line) and measured (red line) transmissions of the metamaterial sample. (b) Retrieved permittivity of the metamaterial layer.

strate at a thickness of  $500\ \mu\text{m}$  using conventional photolithographic methods. The ELC resonators consist of 30 nm thick titanium, 40 nm thick platinum, and 200 nm thick gold layers on top of the GaAs substrate, in which the titanium forms an adhesion layer, and platinum is used to prevent intermetallic diffusion between the titanium and the gold. A photomicrograph of the metamaterial sample is shown in Fig. 1 (right), which demonstrates the high fabrication quality achieved.

Transmission of the metamaterial sample was characterized using a Fourier transform infrared spectrometer at room temperature. In the measurement, a mercury arc lamp produces terahertz waves which are linearly polarized before impinging upon the sample and reference (an open aperture of 3 mm diameter) at normal incidence, before being detected by a liquid helium silicon bolometer. The spectrum of the transmitted intensity is obtained directly through the Fourier transform of the both the sample and reference interferograms, and portions of the signal caused by Fresnel reflections are removed. The transmission (division of the sample by the reference spectra) of the metamaterial sample thus obtained is shown in Fig. 2(a) (red line). There are two transmission minima at 0.95 and 1.44 THz with transmission of 1.2% and 15%, respectively. Between the two resonances, there is a peak at 1.28 THz with a transmission of 44.5%.

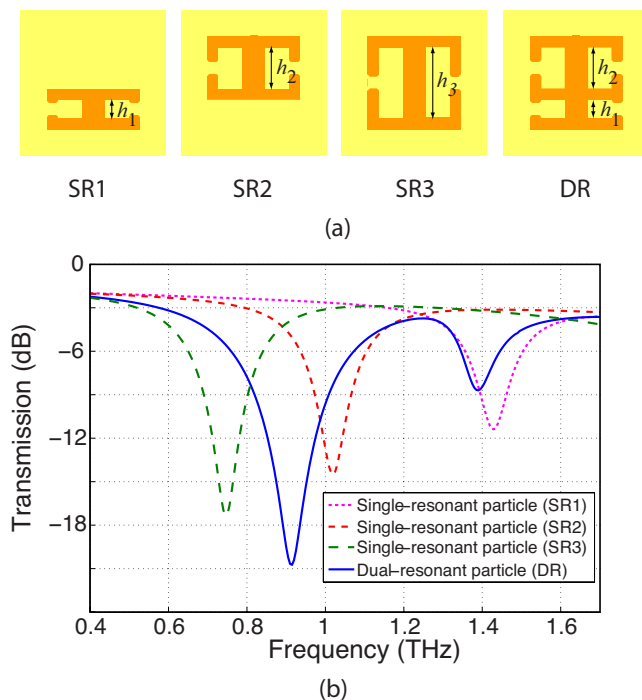


FIG. 3. (Color online) (a) Single-resonant particles SR1, SR2, SR3, and dual-resonant particle DR ( $h_1=6\ \mu\text{m}$ ,  $h_2=14\ \mu\text{m}$ , and  $h_3=24\ \mu\text{m}$ ). (b) Calculated transmission of the metamaterial composed of SR1, SR2, SR3 (pink, red, and green dashed lines, respectively), and DR (blue solid line).

Near the first resonance, a low transmission and a broad stop band are obtained. Compared to the measurement, the errors of the simulation for the transmission minimum frequencies and the peak frequency are 3.7%, 3.5%, and 2.3%, respectively, and the agreement between the simulated and the measured transmission is excellent.

To better understand the significant asymmetry of the two resonances, several comparable single resonance particle metamaterials, as illustrated in Fig. 3(a), are simulated for comparison. These are the particles that comprise the lower part (SR1), the upper part (SR2), and the total part (SR3) of the dual resonance particle, respectively. The calculated transmissions for these single resonance metamaterials are shown in Fig. 3(b) (dashed lines). Their resonant frequencies are 1.43 THz (SR1), 1.02 THz (SR2), and 0.75 THz (SR3), respectively, and the transmission resonances exhibit significant increase in resonance strength from SR1, SR2 to SR3 that is related to the particle size and thus the overall resonator strength of the material.

The calculated transmission of the dual-resonant particle (denoted as DR hereafter), which is a combination of SR1 and SR2, is replotted in Fig. 3(b) (solid line) in decibels. Compared to the resonances of the individual single-resonant particles SR1 and SR2, there is a modest frequency shift for both of the two resonant frequencies of the dual-resonant metamaterial, which is expected from the coupling of these resonances. More importantly, the transmission minimum for the first resonance is  $-20.8\ \text{dB}$ , which is 6.2 dB less than its single resonance counterpart SR2. This indicates that the resonance coupling has increased the response strength of this lower resonance at the expense of the upper resonance. Note that similar shapes of all of the transmission minima suggest that the resonance quality factors are all approxi-

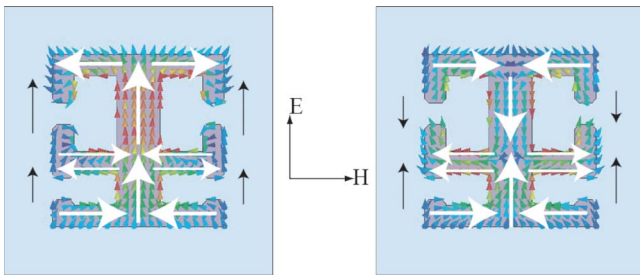


FIG. 4. (Color online) (Left) Near the first resonance, the resonant particle part (upper part) induces the same-direction circular surface current on the nonresonant part (lower part). (Right) Near the second resonance, the resonant particle part (lower part) induces the opposite-direction circular surface current on the nonresonant part (upper part). The wave polarization is shown, and white and black arrows denote the surface current directions and the dipole moments in the gaps, respectively.

mately equal, and thus it is likely the oscillator strength that drives one minimum lower than another.

Remarkably, this transmission minimum is even 3.4 dB deeper than for SR3, which is a single-resonant particle with the same overall size as the DR particle and thus might be expected to have a comparable or larger response strength than both of the DR resonances. This enhanced resonance strength is also reflected in the stop band bandwidths of the different particles. The full width half power bandwidths, defined as 3 dB below the background transmission level of approximately  $-3$  dB, are 0.17, 0.19, and 0.32 THz for the SR2, SR3, and first DR resonance, respectively. Thus the DR metamaterial bandwidth is almost a factor of 2 larger than that obtainable in an identically sized and conventional single resonance metamaterial. This indicates that resonance coupling can be exploited to increase the metamaterial response strength beyond what is easily obtainable in a single resonance material.

An explanation of this resonance enhancement is evident in simulations for the modified response strength of the DR metamaterial with respect to their single-resonant counterparts SR1 and SR2. For the DR particle, the electric response strength is determined by the summation of polarizabilities of the individual resonant parts. Due to the mutual coupling between the single-resonant parts within the dual-resonant particle, the resonant part induces a circular surface current on each part the nonresonant particle part near the resonances, as demonstrated in Fig. 4. The electric response of the particle originates in the electric dipole moments created across the gaps in the particle, and the relative sign of each of these dipole moments is directly linked to the sign of the current at the edges of the gap.

It can be seen that near the first resonant frequency [Fig. 4 (left)], the upper portion of the resonant particle (SR2) contains currents of the same direction as those in the lower part (SR1), leading to parallel dipole moments and thus a strengthening of the resonance as a result of particle dipole moment coupling. Near the second resonant frequency [Fig. 4 (right)], however, the lower part of the resonant particle

(SR1) contains currents with the opposite sense of those in the upper part (SR2), and thus the electric response is weakened due to the partial cancellation of the particle electric dipole moments. For the single-particle dual-resonant metamaterial DR, the geometric filling fractions of the single-resonant particles (SR1 and SR2) on the metamaterial plane do not change, therefore, the electric response for the first resonance of the dual-resonant metamaterial is strengthened. This strong resonance coupling can be an advantage or disadvantage compared to a two particle DR metamaterial. Compared to our previously published dual-band metamaterial,<sup>14</sup> the transmission and permittivity asymmetry are much higher in the single-particle metamaterial. However, the stronger resonance has a much deeper transmission null (by 6 dB) than the responses reported in Ref. 14.

In conclusion, we present a dual-band terahertz metamaterial composed of single geometry ELC resonators that have two distinct resonances. Due to the mutual coupling between the different resonances in the particle, the lower frequency resonance of this metamaterial is stronger than that in a metamaterial composed of identically sized single resonant particles, leading to a larger insertion loss and broader bandwidth. This feature can be exploited in metamaterial design to provide improved material performance in the terahertz regime, and other frequency ranges as well.

The authors are grateful to Dr. Hongsheng Chen at Zhejiang University, for useful discussions.

- <sup>1</sup>R. A. Shelby, D. R. Smith, and S. Schultz, *Science* **292**, 77 (2001).
- <sup>2</sup>J. B. Pendry, A. J. Holden, W. J. Stewart, and I. Youngs, *Phys. Rev. Lett.* **76**, 4773 (1996).
- <sup>3</sup>J. B. Pendry, A. J. Holden, D. Robbins, and W. J. Stewart, *IEEE Trans. Microwave Theory Tech.* **47**, 2075 (1999).
- <sup>4</sup>H. Chen, L. Ran, J. Huangfu, X. Zhang, K. Chen, T. M. Grzegorzczak, and J. A. Kong, *Phys. Rev. E* **70**, 057605 (2004).
- <sup>5</sup>H. Chen, L. Ran, J. Huangfu, X. Zhang, K. Chen, T. M. Grzegorzczak, and J. A. Kong, *Appl. Phys. Lett.* **86**, 151909 (2004).
- <sup>6</sup>D. Schurig, J. J. Mock, and D. R. Smith, *Appl. Phys. Lett.* **88**, 041109 (2006).
- <sup>7</sup>D. Schurig, B. J. Justice, S. A. Cummer, J. B. Pendry, A. F. Starr, and D. R. Smith, *Science* **314**, 977 (2006).
- <sup>8</sup>H. T. Chen, W. J. Padilla, J. M. O. Zide, A. C. Gossard, A. J. Taylor, and R. D. Averitt, *Nature (London)* **444**, 597 (2006).
- <sup>9</sup>W. J. Padilla, M. T. Aronsson, C. Highstrete, M. Lee, A. J. Taylor, and R. D. Averitt, *Phys. Rev. B* **75**, 041102 (2007).
- <sup>10</sup>H. Chen, L. Ran, J. Huangfu, X. Zhang, K. Chen, T. M. Grzegorzczak, and J. A. Kong, *J. Appl. Phys.* **96**, 5338 (2004).
- <sup>11</sup>D. Wang, L. Ran, B. I. Wu, H. Chen, J. Huangfu, T. M. Grzegorzczak, and J. A. Kong, *Opt. Express* **14**, 12288 (2006).
- <sup>12</sup>D.-H. Kwon, D. H. Werner, A. V. Kildishev, and V. M. Shalaev, *Opt. Express* **15**, 1647 (2007).
- <sup>13</sup>U. K. Chettiar, A. V. Kildishev, H.-K. Yuan, W. Cai, S. Xiao, V. P. Drachev, and V. M. Shalaev, *Opt. Lett.* **32**, 1671 (2007).
- <sup>14</sup>Y. Yuan, C. Bingham, T. Tyler, S. Palit, T. Hand, W. J. Padilla, D. R. Smith, N. M. Jokerst, and S. A. Cummer, *Opt. Express* **16**, 9746 (2008).
- <sup>15</sup>D. R. Smith, S. Schultz, P. Marko, and C. M. Soukoulis, *Phys. Rev. B* **65**, 195104 (2002).
- <sup>16</sup>X. Chen, T. M. Grzegorzczak, B. I. Wu, J. Pacheco, and J. A. Kong, *Phys. Rev. E* **70**, 016608 (2004).